KIR2DS2 Expression Identifies NK Cells With Enhanced Anticancer Activity

Matthew D. Blunt, Andres Vallejo Pulido, Jack G. Fisher, Lara V. Graham, Amber D. P. Doyle, Rebecca Fulton, Matthew J. Carter, Marta Polak, Peter W. M. Johnson, Mark S. Cragg, Francesco Forconi and Salim I. Khakoo

J Immunol 2022; 209:379-390; Prepublished online 29 June 2022;
doi: 10.4049/jimmunol.2101139
http://www.jimmunol.org/content/209/2/379

The Journal of Immunology is published twice each month by
The American Association of Immunologists, Inc.,
1451 Rockville Pike, Suite 650, Rockville, MD 20852

Print ISSN: 0022-1767 Online ISSN: 1550-6606.

KIR2DS2 Expression Identifies NK Cells With Enhanced Anticancer Activity

Matthew D. Blunt,*,[1] Andres Vallejo Pulido,*,[1] Jack G. Fisher,* Lara V. Graham,* Amber D. P. Doyle,* Rebecca Fulton,* Matthew J. Carter,† Marta Polak,* Peter W. M. Johnson,† Mark S. Cragg,† Francesco Forconi,† and Salim I. Khakoo*

NK cells are promising cellular therapeutics against hematological and solid malignancies. Immunogenetic studies have identified that various activating killer cell Ig-like receptors (KIRs) are associated with cancer outcomes. Specifically, KIR2DS2 has been associated with reduced incidence of relapse following transplant in hematological malignancies and improved outcomes in solid tumors, but the mechanism remains obscure. Therefore, we investigated how KIR2DS2 expression impacts NK cell function. Using a novel flow cytometry panel, we show that human NK cells with high KIR2DS2 expression have enhanced spontaneous activation against malignant B cell lines, liver cancer cell lines, and primary chronic lymphocytic leukemia cells. Surface expression of CD16 was increased on KIR2DS2^{high} NK cells, and, accordingly, KIR2DS2^{high} NK cells had increased activation against lymphoma cells coated with the clinically relevant anti-CD20 Abs rituximab and obinutuzumab. Bulk RNA sequencing revealed that KIR2DS2^{high} NK cells have upregulation of NK-mediated cytotoxicity, translation, and FCGR gene pathways. We developed a novel single-cell RNA-sequencing technique to identify KIR2DS2^{+} NK cells, and this confirmed that KIR2DS2 is associated with enhanced NK cell–mediated cytotoxicity. This study provides evidence that KIR2DS2 marks a population of NK cells primed for anticancer activity and indicates that KIR2DS2 is an attractive target for NK-based therapeutic strategies. ***The Journal of Immunology*****, 2022, 209: 379–390.**

Natural killer cells are powerful effector cells in the anticancer immune response and act via direct recognition and killing of tumor cells, promotion of adaptive immune responses, and Ab-dependent cellular cytotoxicity (ADCC) (1–3). There is intense interest in targeting NK cells for cancer therapy via adoptive cellular therapies as well as via Ab- and cytokine-mediated stimulation (1, 3, 4).

NK cells are regulated by the integration of signals from an array of nonrearranged activating and inhibitory receptors, of which the killer cell Ig-like receptors (KIRs) are an important component (5). Both KIR and NKG2A/C interact with HLA class I molecules, and the inhibitory KIRs have been well described to sense downregulation of HLA class I and generate inhibitory signals (5). In contrast, there is much less understanding of how activating KIRs regulate the activity of NK cells against cancer cells. This is important because there is more population diversity in expression of activating KIRs than their inhibitory counterparts and thus in the innate genetic susceptibility to cancer (6). Difficulties in understanding the activating KIRs have primarily been caused by a lack of Abs able to sufficiently discriminate from inhibitory KIRs with high sequence homology (6–8). In addition, activating KIR ligands have been hard to define (6) because of a lower affinity for HLA class I compared with inhibitory KIRs (6, 9). Thus, the study of KIR2DS2 has previously been limited in part by a lack of available Abs able to discriminate KIR2DS2 from the closely related inhibitory KIRs KIR2DL3 and KIR2DL2. We have recently shown, however, that KIR2DS2 binds HLA-C in combination with viral peptides containing an alanine and threonine at the carboxy-terminal −1 and −2 of the peptide (10) and developed an Ab combination able to detect NK cells enriched for KIR2DS2 relative to KIR2DL3 and KIR2DL2 (11). In addition, with the use of a reporter cell line, KIR2DS2 has been shown to recognize a β_2-microglobulin–independent ligand on cancer cells (12).

There is substantial diversity in the number of KIR genes that individuals have, and these are encoded as two haplotypes (13). The KIR A haplotype consists of predominantly inhibitory KIR and one activating KIR (KIR2DS4), whereas the KIR B haplotype encodes a more variable gene content that includes more activating KIRs (KIR2DS1, KIR2DS2, KIR2DS3, KIR2DS5, and KIR3DS1). KIR gene diversity has been implicated in antitumor responses in a number of genetic studies, with the KIR B haplotype associated with improved outcome in hematological malignancies following transplant treatment (14–18). In addition, activating KIRs are associated with protection against the development of childhood acute lymphoblastic leukemia (ALL) (19), with the greatest reduction in risk

*School of Clinical and Experimental Sciences, University of Southampton, Southampton, United Kingdom; and †School of Cancer Sciences, University of Southampton, Southampton, United Kingdom

[1]M.D.B. and A.V.P. contributed equally to this work.

ORCIDs: 0000-0003-1099-3985 (M.D.B.); 0000-0002-4688-0598 (A.V.P.); 0000-0002-5090-7503 (J.G.F.); 0000-0003-3235-5570 (A.D.P.D.); 0000-0003-2878-476X (M.P.); 0000-0003-2306-4974 (P.W.M.J.); 0000-0003-2077-089X (M.S.C.); 0000-0002-2211-1831 (F.F.).

Received for publication December 2, 2021. Accepted for publication May 8, 2022.

This work was supported by a John Goldman Fellowship from Leukaemia UK to M.D.B. and grants from the Medical Research Council (519241101) and Cancer Research UK consortium "HUNTER" to S.I.K. The 10X Chromium Controller was funded by a Cancer Research UK Advanced Clinician Scientist Fellowship to Sean Hua Lim (A27179).

Address correspondence and reprint requests to Dr. Matthew D. Blunt, School of Clinical and Experimental Sciences, Level E, South Academic Block, Southampton General Hospital, University of Southampton, Southampton, SO16 6YD, UK. E-mail address: m.d.blunt@soton.ac.uk

The online version of this article contains supplemental material.

Abbreviations used in this article: ADCC, Ab-dependent cellular cytotoxicity; ALL, acute lymphoblastic leukemia; CLL, chronic lymphocytic leukemia; Cy7, cyanine 7; DLBCL, diffuse large B cell lymphoma; KIR, killer cell Ig-like receptor; RAGE-seq, repertoire and gene expression by sequencing; scRNAseq, single-cell RNA sequencing; UMI, unique molecular identifier.

by activating KIRs for developing ALL conferred by KIR2DS2. Expression of KIR2DS2 on donor cells during transplant has also been shown to significantly improve progression-free survival and reduce relapse rates in patients with hematological malignancies, including non-Hodgkin lymphoma (14, 20). In accordance with this, cord blood–derived NK cells with a KIR2DS2-positive genotype showed increased activation against K562 targets cells in vitro as compared with KIR2DS2-negative NK cells (20). In addition, KIR2DS2 is associated with increased activation against glioblastoma cells (21) and improved clinical response in breast cancer, colorectal cancer, non–small cell lung cancer, and hepatocellular carcinoma (22–25). However, these studies have been unable to discriminate between KIR2DS2 and the closely related inhibitory KIRs KIR2DL3 and KIR2DL2 because of the strong linkage disequilibrium between KIR2DS2 and KIR2DL2 in genetic studies and a lack of discriminatory Abs in functional studies.

NK cells are also important determinants of treatment success with mAbs. Anti-CD20 Ab therapies have revolutionized the treatment of B cell malignancies, and ADCC mediated by NK cells is thought to contribute to the therapeutic response (26–28). NK cells express the Fc receptor CD16, enabling them to execute ADCC (28). KIR2DS2-positive NK cells have enhanced CD16 expression compared with KIR2DS2-negative NK cells (21), and the presence of KIR2DS2 is associated with enhanced ADCC to anti-GD_2 and prolonged event-free survival during anti-GD_2 treatment for neuroblastoma (29). Whether KIR2DS2 affects NK cell activation in response to anti-CD20 Abs, however, is unknown. This is important, given the beneficial role of activating KIRs in patients with hematological malignancies and in the requirement for identification of highly active subsets of NK cells to improve response to immunotherapies. Here, we used our recently developed flow cytometry–based discrimination technique (11) and novel single-cell RNA-sequencing (scRNAseq) approach in which coupled KIR sequencing occurs to investigate the potential basis of the enhanced activity of KIR2DS2$^+$ NK cells against cancer targets.

Materials and Methods

Samples and cell lines

Healthy donor PBMCs were obtained with full ethical approval from the National Research Ethics Committee (reference 06/Q1701/120) and cryopreserved in liquid nitrogen until use. Chronic lymphocytic leukemia (CLL) samples were obtained from patients attending Southampton General Hospital following written informed consent and in accordance with ethics committee approvals (UK National Research Ethics Service number 19/WM/0262) and the Declaration of Helsinki. CLL patient PBMCs were obtained and cryopreserved in liquid nitrogen until use.

Cell lines used as targets in functional assays were as follows: Mino, DOHH2, REH, Ramos, HBL-1, SU-DHL-6, SU-DHL-4, Raji, JeKo-1, Granta-519, MAVER-1, the HLA-null transformed B lymphoblastoid cell line 721.221, SNU-398, HepG2, and PLC/PRF/5. All cell lines were cultured in RPMI 1640 medium supplemented with 1% penicillin-streptomycin (Life Technologies) and 10% heat-inactivated FBS (Sigma-Aldrich).

Staining of cells for flow cytometry

Healthy PBMCs or isolated NK cells (average purity of 96% NK cells achieved using the Miltenyi Biotec NK isolation kit) were blocked with 10% AB serum for 20 min at 4°C, then washed and stained with Abs for 30 min at 4°C in FACS buffer (PBS, BSA 1%, sodium azide 0.05%). Surface Abs used were REA147-FITC (Miltenyi Biotec), CH-L-PE (BD Biosciences), CD56-PE/cyanine 7 (Cy7) (BioLegend), CD3-PerCP (BioLegend), and CD16-allophycocyanin (BioLegend). Cells were then washed in FACS buffer and analyzed by flow cytometry using a BD FACSAria device. Analysis was performed using FlowJo version 10 software. For HLA-C staining, B cell lines were incubated with DT9 Ab for 30 min in FACS buffer, then washed in FACS buffer and stained with antimouse secondary Ab Alexa Fluor 647. Cells were then analyzed by flow cytometry using a BD Accuri device, and data were analyzed using FlowJo version 10.

NK cell degranulation assay

Healthy donor PBMCs or isolated NK cells were stimulated overnight with IL-15 (1 ng/ml; R&D Systems) and coincubated with target cells at 10:1, 5:1, or 1:1 E:T ratio as indicated for 4 h with anti-CD107a Alexa Fluor 647. For assays using primary CLL cells as targets, CLL cells were isolated using a B-CLL isolation kit (Miltenyi Biotec) before coincubation with healthy donor PBMCs. For assays in combination with anti-CD20 Abs, target cells were incubated with indicated Ab (1 μg/ml; in-house) for 20 min at 4°C before addition of PBMCs or purified NK cells (Miltenyi Biotec NK isolation kit) at a 10:1 E:T ratio. Excess anti-CD20 Ab in the medium was removed by two washes with RPMI media before addition of PBMCs. GolgiStop (BD Biosciences) was added 1 h after coincubation, and cells were then stained with REA147-FITC (Miltenyi Biotec), CH-L-PE (BD Biosciences), CD56-PE/Cy7 (BioLegend), and CD3-PerCP (BioLegend) and analyzed by flow cytometry on a BD FACSAria device. Data were analyzed using FlowJo version 10 software.

Intracellular cytokine staining of human cells

Healthy donor PBMCs were stimulated overnight with IL-15 (1 ng/ml) and then coincubated with target cells at a 5:1 E:T ratio for 4 h. GolgiStop (BD Biosciences) was added 1 h after coincubation, and cells were then stained for surface markers REA147-FITC (Miltenyi Biotec), CH-L-PE (BD Biosciences), CD56-PE/Cy7 (BioLegend), and CD3-PerCP (BioLegend). Cells were then fixed and permeabilized, stained for IFN-γ BV421 (BioLegend) and TNF-α Alexa Fluor 700 (BioLegend), and analyzed by flow cytometry on a BD FACSAria device. Data were analyzed using FlowJo version software.

Bulk RNA sequencing

KIR2DS2^{high}, KIR2DL3/L2^{high}, and KIR2DL3/L2/S2$^-$CD56^{dim}CD3$^-$ healthy human cells were sorted using a BD FACSAria and the above-described surface staining protocol with Abs REA147-FITC, CH-L-PE, CD56-PE/Cy7, and CD3-PerCP. RNA was subsequently isolated using the RNeasy Kit (QIAGEN) according to the manufacturer's instructions. All samples were subjected to an indexed paired-end sequencing run of 2 × 150 cycles on an Illumina NovaSeq 6000 at 20 million reads per sample. Paired-end sequence reads were quantified to transcript abundance using Kallisto (30) with bias correction and 50 bootstrap samples. Reads were mapped to ENSEMBL release 95. On average, the percentage of exonic aligned reads was 56.5%. The transcript abundance was then summarized to gene level using Sleuth (31).

Raw counts from RNA sequencing were processed in the Bioconductor package EdgeR (32), and variance was estimated and size factor normalized using trimmed mean of M-values. Genes with a minimum of two reads at a minimum of 50% samples were included in the downstream analyses. All fit models included a term to model individual variation. For the identification of differentially expressed genes among the three groups (KIR2DS2^{high}, KIR2DL3/L2^{high}, and KIR2DL3/L2/S2$^-$), a paired model was used in all the possible pairs. Genes with a false discovery rate–corrected p value <0.05 resulting from a likelihood ratio test using a negative binomial generalized linear model fit were identified as differentially expressed. Gene ontology and pathway enrichment analyses were conducted using Camera (33) and Ensemble of Gene Set Enrichment Analyses (34).

scRNAseq

Single-cell libraries were generated using the Chromium Single Cell 3′ Library and Gel Bead Kit version 3.1 from 10× Genomics. Briefly, single-cell suspensions were tagged using TotalSeq hashtag Abs (BioLegend). After pooling, 10,000 cells were loaded onto a channel of the 10× chip to produce Gel Bead-in-Emulsions. This underwent reverse transcription to barcode RNA before cleanup and cDNA amplification followed by enzymatic fragmentation and 5′ adaptor and sample index attachment. Libraries were sequenced on the NextSeq 500 system (Illumina) with 28 × 60–bp paired-end sequencing.

KIR long-read sequencing

KIR molecules were enriched and sequenced using a modified repertoire and gene expression by sequencing (RAGE-seq) protocol (35). Briefly, 3 ng of full-length cDNA from the short-read experiment was amplified by PCR using KAPA HotStart HIFI ReadyMix (KAPA Biosystems) with the following cycling conditions: 98°C for 3 min; [98°C for 20 s, 65°C for 30 s, 72°C for 2 s] × 10 cycles 72°C for 3 min. After purification with AMPure beads (Beckman Coulter), samples were incubated at 65°C to produce ssDNA, and then KIR molecules were captured using a pool of custom-designed probes (Table I). Washes were done following the xGen hybridization capture protocol (Integrated DNA Technologies). Captured molecules were amplified by

Table I. Custom probes used for KIR detection

Gene	Sequence	Scale	Purification
KIR2DL3	5′-/5BiosG/CATCCTGCAATGTTGGTCAGATGTCAGGTTTCAGCACTTCCTTC TGCACAGAGAAGGGAAGTTTAAGGACACTTTGCACCTCATTG-3′	4 nmol	Standard desalting
KIR2DS2	5′-/5BiosG/GAACAGCGAGGATTCTGATGAACAAGACCATCAGGAGGTGT CATACGCATAATTGGATCACTGTGTTTTCACACAGAGAGAAATCA-3′	4 nmol	Standard desalting
KIR2D2	5′-/5BiosG/GCCGCCTGTCTGCACAGACAGCACCATGTCGCTCATGGTCGT CAGCATGGCGTGTGTTGGGTTCTTCTTGCTGCAGGGGGCCTGGCCAC-3′	4 nmol	Standard desalting
KIR2D3	5′-/5BiosG/GCCTTCACCCACTGAACCAAGCTCCAAAACCGGTAACCCCAG ACACCTGCATGTTCTGATTGGGACCTCAGTGGTCAAAATCCCTTTCA-3′	4 nmol	Standard desalting

PCR and purified using the same procedure as before. Nanopore libraries were prepared using the LSK-110 kit and sequenced on a MinION flow cell (R9.4.1).

Bioinformatic analysis

For short-read alignment, read filtering, barcode, and unique molecular identifier (UMI) counting were performed using Cell Ranger version 6.0. High-quality barcodes were selected based on the overall UMI distribution using emptyDrops (36). All further analyses were run using the Python-based scanpy (37). To remove low-quality cells, we filtered cells with a high fraction of counts from mitochondrial genes (20% or more) indicating stressed or dying cells (38). In addition, genes expressed in fewer than 20 cells were excluded. Cell by gene count matrices of all samples were concentrated to a single matrix, and values were log transformed. To account for differences in sequencing depth or cell size, UMI counts were normalized using variance-stabilizing transformation. The top variable genes were selected based on normalized dispersion. This output matrix was input to all further analyses, except for differential expression testing, where all genes were used.

For long reads, raw Nanopore data were base called using Guppy (version 4.4.2) with Google Colab. The base-called reads were processed to remove low-quality reads and to extract reads containing barcodes and UMI sequences matching the Illumina library using Sicelore (39). Quality control passing reads were demultiplexed using the top barcodes from the short-read data (35). Single-cell individual FASTQ files were mapped against the IPD-KIR sequence database (40, 41) using minimap2 (version 2.17) with the parameters "-ax map-ont -p 0 -N 10" to keep multimapping reads. Transcript abundance was estimated using the expectation-maximization approach algorithm (Nanocount) (42). Output abundance data were compiled and collapsed by gene name using custom Python scripts and further analyzed using scanpy (37). Nanopore data were integrated to the short-read data by sharing the Uniform Manifold Approximation and Projection representation coordinates.

Statistical analysis

For experimental data, statistical analysis was performed using GraphPad Prism 8.0 software. Normal distribution of data was evaluated by the Shapiro-Wilk test, and statistical significance was determined using Student two-tailed *t* test, Wilcoxon signed-rank test, or two-way ANOVA as appropriate. Data were considered statistically significant at $p < 0.05$.

Results

KIR2DS2^{high} NK cells have enhanced activation against malignant cells

The presence of the gene for KIR2DS2 within an individual is associated with improved clinical responses in patients with B cell malignancies (19, 20). To investigate the basis for this association, we investigated, at a functional level, the relationship between the expression of KIR2DS2 and activation of NK cells against a number of malignant B cell lines. We used the recently described Ab combination of REA147 and CH-L to separate CD3$^-$CD56^{dim} NK cells based on high expression of KIR2DS2 (KIR2DS2^{high}), high expression of KIR2DL3/L2 with or without KIR2DS2 (KIR2DL3/L2^{high}), or no expression of KIR2DL3, KIR2DL2, and KIR2DS2 (KIR2DL3/L2/S2$^-$) as indicated in Fig. 1A (11). CH-L has been reported to bind KIR2DS2, KIR2DL3, and KIR2DL2, whereas REA147 preferentially binds KIR2DL2 and KIR2DL3 compared with KIR2DS2 (11). Degranulation (CD107a) was used as a readout of NK cell activation against malignant B cells in combination with this Ab panel (Fig. 1A).

KIR2DS2^{high} NK cells had significantly enhanced activation in comparison with both KIR2DL3/L2^{high} and KIR2DL3/L2/S2$^-$ NK cells against DOHH2 cells (derived from diffuse large B cell lymphoma [DLBCL]) ($p < 0.0001$ and $p < 0.001$, respectively) (Fig. 1A, 1B). We further tested NK cell activation against a panel of B cell lines encompassing mantle cell lymphoma (Mino, Maver-1, Granta-519), Burkitt lymphoma (Ramos, Raji), activated B cell DLBCL (HBL-1), germinal center B cell DLBCL (SU-DHL-6, SU-DHL-4), and ALL (REH) (Fig. 1B). These data showed that KIR2DS2^{high} NK cells had higher activation than KIR2DL3/L2^{high} NK cells against all B cell lines tested, as well as higher activation than KIR2DL3/L2/S2$^-$ cells against all cell lines apart from MAVER and Granta-519. To test KIR2DS2^{high} NK cell activation against primary tumor cells, we used peripheral blood–derived CLL cells from five different patients as targets. KIR2DS2^{high} NK cells had significantly increased activation against CLL cells as compared with other NK cell subgroups, KIR2DL3/L2^{high} ($p < 0.001$) and KIR2DL3/L2/S2$^-$ ($p < 0.05$) (Fig. 1C, 1D). Together these data demonstrate that KIR2DS2 marks a population of NK cells with enhanced potential for response against malignant B cells.

To test whether this effect was dependent on HLA-C expression by target cells, we used the HLA-null transformed B cell line 721.221 as target cells. In the absence of HLA-C expression on target cells, both KIR2DS2^{high} and KIR2DL3/L2^{high} NK cells showed significantly enhanced activation compared with KIR2DL3/L2/S2$^-$ NK cells, consistent with the licensing effect of KIR (Fig. 1E). However, KIR2DS2^{high} cells showed increased activation ($p < 0.05$) compared with KIR2DL3/L2^{high} cells in the absence of HLA-C (Fig. 1E), indicating that the enhanced activation of KIR2DS2^{high} compared with KIR2DL3/L2^{high} cells is not solely due to a lack of inhibition mediated by KIR2DL3/L2. In accordance with this, KIR2DS2^{high} NK cells showed enhanced degranulation in the presence of both high HLA-C–expressing (JeKo-1) and low HLA-C–expressing (DOHH2) cell lines (Supplemental Fig. 1). In addition, KIR2DS2^{high} NK cells showed superior activation against targets cells with different HLA-C genotypes (Table II) compared with KIR2DL3/L2^{high} and KIR2DL3/L2/S2$^-$ NK cells. These data indicate that KIR2DS2 marks a population of NK cells with enhanced effector function and that this activity is agnostic to HLA-C expression on target cells. Baseline degranulation in the absence of target cells was similar between KIR2DS2^{high} cells and KIR2DL3/L2/S2$^-$ NK cells and only marginally higher (<2%) than KIR2DL3/L2^{high} NK cells (Supplemental Fig. 2A). This indicates that basal levels of NK cell activation do not account for this enhanced response.

NK cells promote adaptive immune responses against cancer via production of cytokines (3), and we therefore sought to determine whether KIR2DS2 also marks a population of NK cells with enhanced cytokine production. In response to the DLBCL cell line DOHH2, KIR2DS2^{high} NK cells had significantly increased

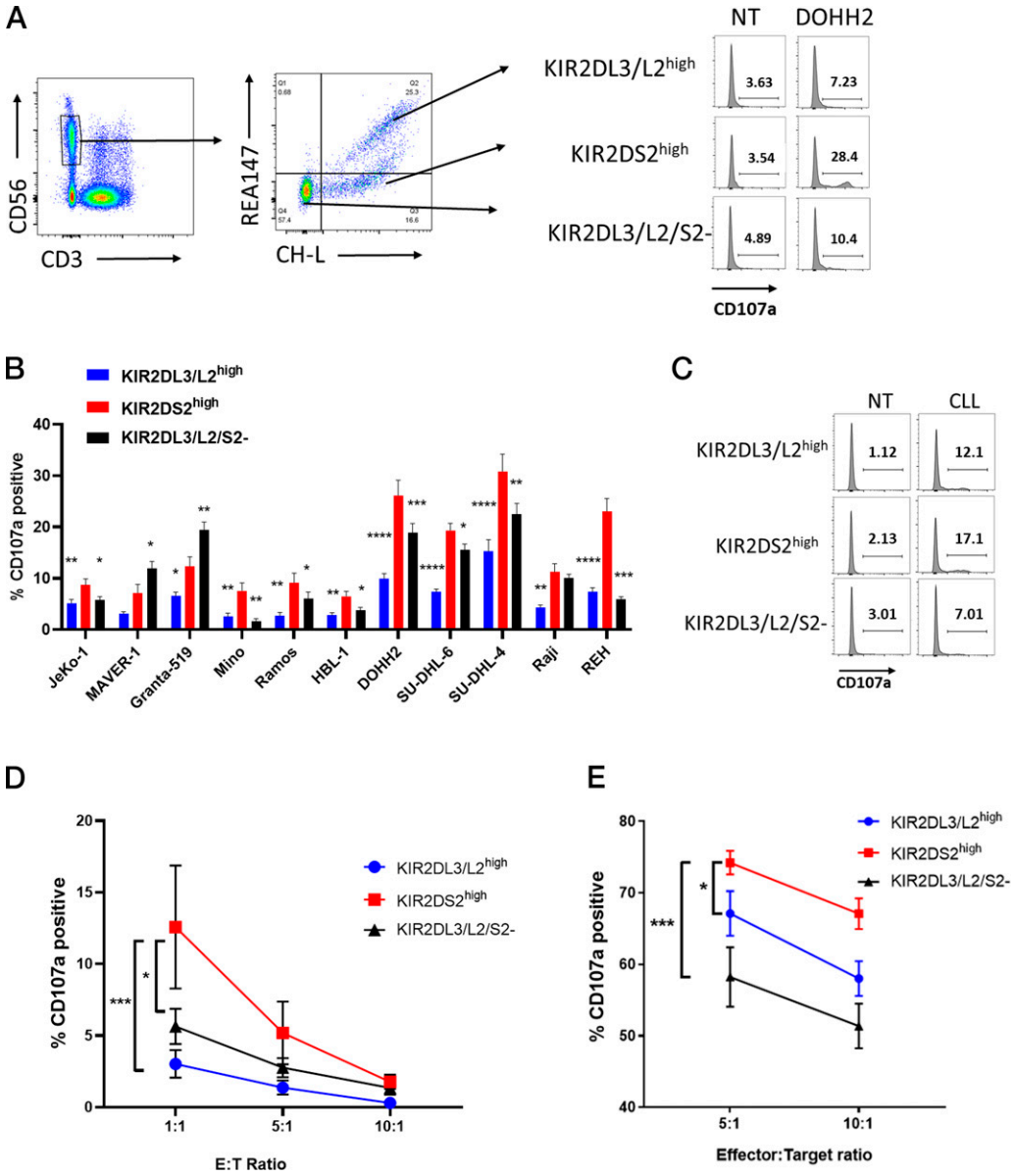

FIGURE 1. KIR2DS2^{high} NK cells have increased activation against malignant B cells. Healthy human PBMCs were incubated with IL-15 (1 ng/ml) overnight and then coincubated with DOHH2, REH, Mino, JeKo-1, MAVER-1, Granta-519, Ramos, HBL-1, SU-DHL-6, SU-DHL-4, or Raji (n = 10–15) cells or no target (NT) at 5:1 E:T ratio for 4 h. CD107a expression was assessed on CD3$^-$CD56^{dim} NK cells separated into KIR2DS2^{high}, KIR2DL3/L2^{high}, or KIR2DL3/L2/S2$^-$ populations using REA147 and CH-L Ab combinations as shown in (**A**). Representative data against DOHH2 are shown in A, and summarized data as mean ± SEM are shown in **B** for each indicated cell line. (**C** and **D**) Healthy human PBMCs from five different donors were incubated with IL-15 (1 ng/ml) overnight and then coincubated with primary human CLL cells from five different donors at 1:1, 5:1, or 10:1 E:T ratio or no target (NT) for 4 h. CD107a expression was assessed on CD3$^-$CD56^{dim} NK cells separated into KIR2DS2^{high}, KIR2DL3/L2^{high}, or KIR2DL3/L2/S2$^-$ populations. Representative data are shown in C, and summarized data are shown as mean ± SEM in D. (**E**) Healthy human PBMCs were incubated with IL-15 (1 ng/ml) overnight and then coincubated with 721.221 (n = 7) cells at 5:1 and 10:1 E:T ratios for 4 h. CD107a expression was assessed on CD3$^-$CD56^{dim} NK cells separated into KIR2DS2^{high}, KIR2DL3/L2^{high}, or KIR2DL3/L2/S2$^-$ populations. *$p < 0.05$, **$p < 0.01$, ***$p < 0.001$, ****$p < 0.0001$.

production of IFN-γ ($p < 0.01$) and TNF-α ($p < 0.01$) compared with KIR2DL3/L2^{high} NK cells and no difference from KIR2DL3/L2/S2$^-$ cells (Fig. 2A, 2B, 2D, 2E). To test whether this was a general effect against different target cells, we then assessed NK cell activation against the ALL-derived cell line REH. KIR2DS2^{high} NK cells had significantly increased production of IFN-γ compared with KIR2DL3/L2/S2$^-$ cells ($p < 0.01$) and significantly increased production of TNF-α compared with both KIR2DL3/L2/S2$^-$ (p = 0.001) and KIR2DL3/L2^{high} cells ($p < 0.05$) (Fig. 2C, 2F). Variability in cytokine production between donors was evident, as previously reported (43); however, KIR2DS2^{high} NK cells were significantly associated with increased cytokine production (Fig. 2). Although average cytokine production detected was less than 10% for both IFN-γ and TNF-α, this is consistent with previous reports for NK cell activation (44, 45). To further test the association of KIR2DS2 with cytokine expression, we used the HLA-C–null cell line 721.221 as targets. In accordance with the previous results, KIR2DS2^{high} NK cells showed increased IFN-γ expression against 721.221 cells compared with KIR2DL3/L2^{high} and KIR2DL3/L2/S2$^-$ NK cells (Supplemental Fig. 2B). In the absence of target cells, there was no significant difference in levels of IFN-γ between the different NK subgroups, and, for TNF-α in the absence of target

Table II. HLA allele expression of target cell lines

Cell Line	HLA-C Allele Typing	Reference (PubMed ID)
JeKo-1	C*14:02 C*14:02	25960936
MAVER-1	C*03:03 C*07:02	25960936
Granta-519	C*06:02 C*07:02	25960936
Mino	C*04:01 C*12:03	25960936
REH	C*06:02 C*04:01	26589293
Raji	C*04:01 C*03:04	25960936
SU-DHL-4	C*03:04 C*03:04	26589293
Ramos	C*16:01 C*16:01	25960936
SU-DHL-6	C*07:06 C*03:03	26589293
DOHH2	C*07:04 C*07:04	25960936
HBL-1	NA	NA
SNU-398	C*04:01 C*01:02	26589293
HepG2	C*16:02 C*04:01	25960936
PLC/PRF/5	C*04:01 C*17:01	26589293
721.221	HLA-C null	3257565

NA, not available.

cells, KIR2DS2^{high} NK cells had significantly lower levels than KIR2DL3/L2/S2^{-} NK cells (Supplemental Fig. 2A).

Taken together, these data indicate that KIR2DS2^{+} NK cells are primed for activation, and, to investigate if this effect was specific to malignant B cell targets, we tested NK cell activation against cell lines derived from patients with hepatocellular carcinoma. KIR2DS2^{high} NK cells showed increased activation in response to SNU-398, HepG2, and PLC/PRF/5 cells compared with KIR2DL3/L2/S2^{-} and KIR2DL3/L2^{high} NK cells (Fig. 3A–C). This confirms that high KIR2DS2 expression marks a population of NK cells with enhanced potential for activation against both solid and hematologic cancer cells compared with NK cells with low or absent expression of KIR2DS2.

KIR2DS2^{high} NK cells have increased CD16 expression and enhanced response to anti-CD20 Abs

To define the impact of this enhanced activation on ADCC, we investigated CD16 expression on KIR2DS2^{high} NK cells by flow cytometry and determined the response of KIR2DS2^{high} NK cells to anti-CD20–coated malignant B cells. KIR2DS2^{high} NK cells from healthy donors had significantly increased expression of CD16 compared with KIR2DL3/L2^{high} and KIR2DL3/L2/S2^{-} NK cells, as measured by both the mean fluorescence intensity of the whole subpopulation and the percentage of CD16^{+} NK cells (Fig. 4A–C). Importantly, CD56^{bright} NK cells were excluded from this analysis, and therefore differences in CD16 expression were not due to the presence of CD56^{bright}CD16^{-} cells within the KIR2DL3/L2/S2^{-} population. We subsequently tested whether increased CD16 expression was associated with enhanced CD16-mediated functional responses. CD56^{dim} NK cell activation was assessed in response to two anti-CD20 Abs currently in clinical use: rituximab and obinutuzumab. Using healthy human PBMC samples, activation of KIR2DS2^{high} NK cells in response to rituximab- and obinutuzumab-coated DOHH2 lymphoma cells was significantly higher than KIR2DL3/L2^{high} and KIR2DL3/L2/S2^{-} NK cells (Fig. 4D, 4E). These results were confirmed using isolated primary human NK cells (Supplemental Fig. 2C).

Because KIR2DS2^{high} NK cells had higher baseline activity than KIR2DL3/L2/S2^{-} cells against DOHH2 cells, we also tested MAVER-1 cells as targets in ADCC assays in which spontaneous KIR2DS2^{high} NK cell activity was lower than that of KIR2DL3/L2/S2^{-} cells (see Fig. 1B). This allowed assessment of CD16 ligation on NK cell activation in the absence of enhanced natural cytotoxicity in the KIR2DS2^{high} population. Consistent with the results for DOHH2 cells, coincubation of MAVER-1 cells with rituximab and obinutuzumab led to superior activation of KIR2DS2^{high} NK cells compared with KIR2DL3/L2^{high} NK cells (Fig. 4F, 4G). The addition of rituximab and obinutuzumab also induced activation of KIR2DS2^{high} NK cells to a level comparable to that of KIR2DL3/L2/S2^{-} NK cells, in contrast to the lower activation of KIR2DS2^{high} NK cells evident in the absence of CD16 ligation (Fig. 4F, 4G). We then tested whether KIR2DS2 was associated with enhanced ADCC against target cells that lack expression of HLA-C by using the HLA-C–null cell line 721.221. In the absence of HLA-C, KIR2DS2^{high} NK cells had significantly increased activation against 721.221 cells compared with KIR2DL3/L2^{high} and KIR2DL3/L2/S2^{-} NK cells in combination with rituximab (Fig. 4H, 4I). In combination with obinutuzumab, KIR2DS2^{high} NK cells showed significantly increased activation against 721.221 cells compared with KIR2DL3/L2/S2^{-} NK cells (Fig. 4H, 4I). Together, these results indicate that KIR2DS2^{high} NK cells possess enhanced reactivity to CD16 ligation in response to anti-CD20 Abs and provide a further functional correlate of KIR2DS2 with beneficial outcomes of cancer.

KIR2DS2^{high} NK cells express a distinct transcriptional profile associated with enhanced cytotoxicity

To identify the mechanisms for this enhanced activity, we performed RNA sequencing of healthy human CD3^{-} CD56^{dim} NK cells sorted by flow cytometry into three subgroups: KIR2DS2^{high}, KIR2DL3/L2^{high}, and KIR2DL3/L2/S2^{-}. In accordance with the flow cytometry panel used (6), KIR2DL3 was significantly enriched in the KIR2DL3/L2^{high} subset compared with KIR2DS2^{high} and KIR2DSL3/L2/S2^{-} cells (Supplemental Fig. 3A) (11). Principal component analysis indicated that KIR2DS2^{high} NK cells had a

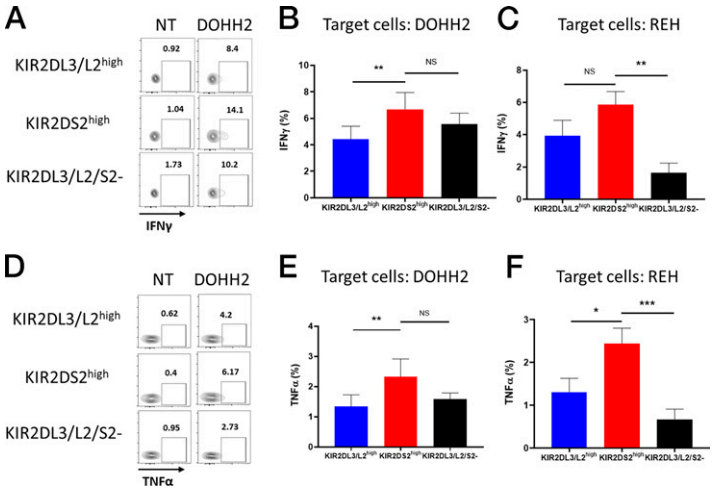

FIGURE 2. Enhanced IFN-γ and TNF-α production by KIR2DS2^{high} NK cells in response to malignant B cells. Healthy human PBMCs were incubated with IL-15 (1 ng/ml) overnight and then coincubated with (**A** and **B**) DOHH2 ($n = 12$) or (**C**) REH ($n = 8$) cells at a 5:1 E:T ratio or no target (NT) for 4 h. Cells were then fixed, permeabilized, and stained for IFN-γ and TNF-α. Expression was assessed on CD3^{-}CD56^{dim} NK cells separated into KIR2DS2^{high}, KIR2DL3/L2^{high}, or KIR2DL3/L2/S2^{-} populations. Representative flow cytometry plots are shown for IFN-γ in A and TNFα in (**D**). Summarized data are presented as mean ± SEM for IFN-γ against DOHH2 cells in B and REH cells in D. Summarized data are presented as mean for TNF-α against DOHH2 cells in (**E**) and REH cells (**F**). *$p < 0.05$, **$p < 0.01$, ***$p < 0.001$.

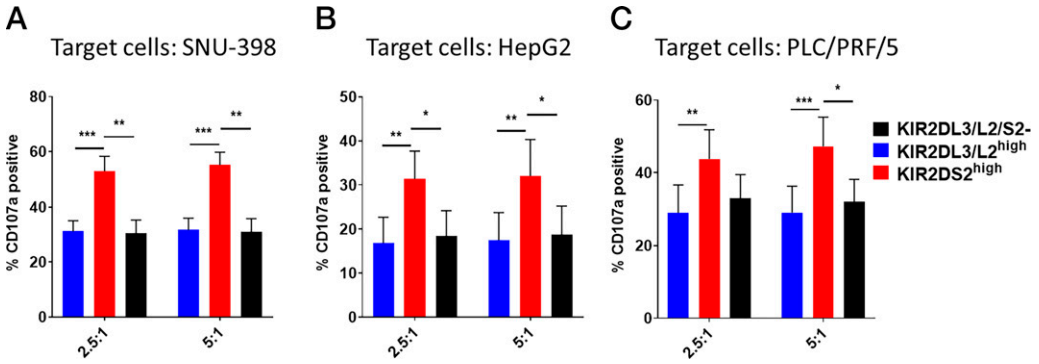

FIGURE 3. KIR2DS2^{high} NK cells have increased activation against liver cancer–derived cell lines. Healthy human PBMCs were incubated with IL-15 (1 ng/ml) overnight and then cocultured with (**A**) SNU-398 ($n = 7$), (**B**) HepG2 ($n = 9$), or (**C**) PLC/PRF/5 ($n = 9$) cells at 2.5:1 or 5:1 E:T ratio for 4 h. CD107a expression was assessed on CD3^{-}CD56^{dim} NK cells separated into KIR2DS2^{high}, KIR2DL3/L2^{high}, or KIR2DL3/L2/S2^{-} populations. Data show mean ± SEM CD107a expression on NK cells. *$p < 0.05$, **$p < 0.01$, ***$p < 0.001$.

distinct transcriptional profile compared with KIR2DL3/L2/S2^{-} and KIR2DL3/L2^{high} NK cells (Fig. 5A). Differentially expressed gene analysis showed that KIR2DS2^{high} NK cells had 1719 significantly altered genes compared with KIR2DL3/L2^{high} cells and 168 significantly altered genes compared with KIR2DL3/L2/S2^{-} NK cells (Fig. 5B). Specific genes of interest associated with NK antitumor responses upregulated in KIR2DS2^{high} compared with KIR2DL3/L2/S2^{-} NK cells included NKG7, granzyme B, and CCL5 (Fig. 5C, 5D, and Supplemental Fig. 3A). Furthermore, consistent with our observations by flow cytometry, there was upregulation of the gene *FCGR3A*, which encodes CD16, and a trend ($p = 0.07$) for upregulation of *FCER1G* (the associated FcRγ signaling subunit) in KIR2DS2^{high} NK cells (Supplemental Fig. 3A). Pathway analysis revealed that KIR2DS2^{high} NK cells compared with KIR2DL3/L2/S2^{-} NK cells have upregulation of pathways, including NK cell–mediated cytotoxicity (Supplemental Fig. 3B) ($p < 0.005$), ribosome, and oxidative phosphorylation (Fig. 5E). These changes could be due to licensing of KIR-expressing cells; however, compared with KIR2DL3/L2^{high} cells, KIR2DS2^{high} NK cells have upregulation of pathways associated with FCGR activation, eukaryotic translation elongation, and eukaryotic translation initiation (Fig. 5F). Increased ribosome and translational activity is consistent with the enhanced ability of KIR2DS2^{high} NK cells to produce cytokines and cytotoxic granules upon recognition of target cells (see Figs. 1–3). These data indicate that KIR2DS2^{high} NK cells express a unique transcriptional profile, enriched for genes associated with NK cell activation and translation, in accordance with our functional data.

scRNAseq confirms that KIR2DS2 is associated with enhanced cytotoxicity

The high sequence similarity among the KIR genes means that many KIR sequencing reads map to multiple genes and are hence discarded by conventional RNA-sequencing pipelines, thereby limiting the power of analysis. Our bulk RNA-sequencing data analysis was performed on populations of NK cells separated using flow cytometry–mediated detection of KIR combinations and hence did not allow discrimination between individual KIRs at the single-cell level. We therefore developed a novel scRNAseq to sequence full-length KIRs based on the RAGE-seq technique (35), which combines short-read transcriptomic profiling with long-read Nanopore sequencing.

scRNAseq analysis performed on cells from four PBMC donors enriched for NK cells yielded 6525 cells following filtering and quality control, of which 72.2% were NK CD16^{hi} cells and 6.7% were NK CD56^{hi} (Fig. 6A). NK CD16^{hi} cells were characterized by the expression of NCR1, CD16, and NKG7 and low levels of CD56, whereas NK CD56^{hi} cells were positive for CD56 and NRC1 and negative for CD16 (Supplemental Fig. 4A). NK cells were annotated as NK CD16^{hi}, NK CD56^{hi}, and NK proliferative subgroups using gene expression markers indicated in Fig. 6B. No significant differences in the frequency of NK subtypes were found among the four donors (Supplemental Fig. 4B). The expression of KIR2DS2 and the closely related inhibitory KIR, KIR2DL3, was successfully detected by Nanopore sequencing and mapped to the NK cell populations defined by short-read transcriptomics (Fig. 6C). We then assessed the relationship between KIR2DS2 and KIR2DL3 expression with the transcriptomic profile of CD16^{hi} (CD56^{dim}) NK cells. Significantly upregulated genes within the KIR2DS2^{+} population compared with KIR2DL3/S2^{-} cells included key NK-related genes (KLRD1, KIR2DL3, NKG7, and granzyme B) (Fig. 6D), which were also evident in the bulk RNA-sequencing results (see Fig. 5 and Supplemental Fig. 3A). Gene set enrichment analysis of KIR2DS2^{+} versus KIR2DS2^{-} CD16^{hi} NK cells revealed that the most significantly upregulated pathway in KIR2DS2^{+} NK cells was NK cell–mediated cellular cytotoxicity (Fig. 6E), confirming our previous functional and bulk RNA-sequencing results. NK cells and T cells share common signaling pathways, and, consistent with an enhanced activation state of KIR2DS2^{+} NK cells, the TCR signaling pathway was also significantly enhanced. In addition, scRNAseq allowed us to then compare the transcriptomic profile of KIR2DS2^{+}KIR2DL3^{-} with KIR2DS2^{+} KIR2DL3^{+} and KIR2DS2^{-}KIR2DL3^{+} CD16^{hi} NK cells, which was not previously possible because of the high sequence homology between these KIR genes. KIR2DS2^{+}KIR2DL3^{+} NK cells were more strongly enriched for NK-mediated cytotoxicity genes than KIR2DS2^{+}KIR2DL3^{-} cells, consistent with NK cell licensing by HLA-C (Fig. 6F). Furthermore, KIR2DS2^{+}KIR2DL3^{-} cells showed significantly greater coexpression of KIR3DL1 than the other NK subgroups (Fig. 6G). A proportion of 50.7% ($n = 394$) of NK cells with long-read sequences coexpressed KIR2DS2 and KIR2DL3, with 17.5% ($n = 136$) expressing only KIR2DS2 and 31.8% ($n = 247$) expressing only KIR2DL3 (Fig. 6G). KIR2DS2^{+}KIR2DL3^{-} cells showed high levels of expression of *KLRD1* (CD94), *RAC2* (a small GTPase), *GZMH* (granzyme H), and *GZMM* (granzyme M), whereas KIR2DS2^{+}KIR2DL3^{+} double-positive cells expressed high levels of *PRF1* (perforin), *HCST* (DAP10), and *KLRK1* (NKG2D) (Fig. 6H). Together, these data confirm that KIR2DS2^{+} NK cells possess a transcriptomic profile associated with enhanced cytotoxicity, in accordance with the functional in vitro data from this study. This is also in accordance with previous immunogenetic studies demonstrating that KIR2DS2 may be associated with protection against cancer (6).

Discussion

In this study, we identify that NK cells with high expression of KIR2DS2 have enhanced effector function against malignant cells

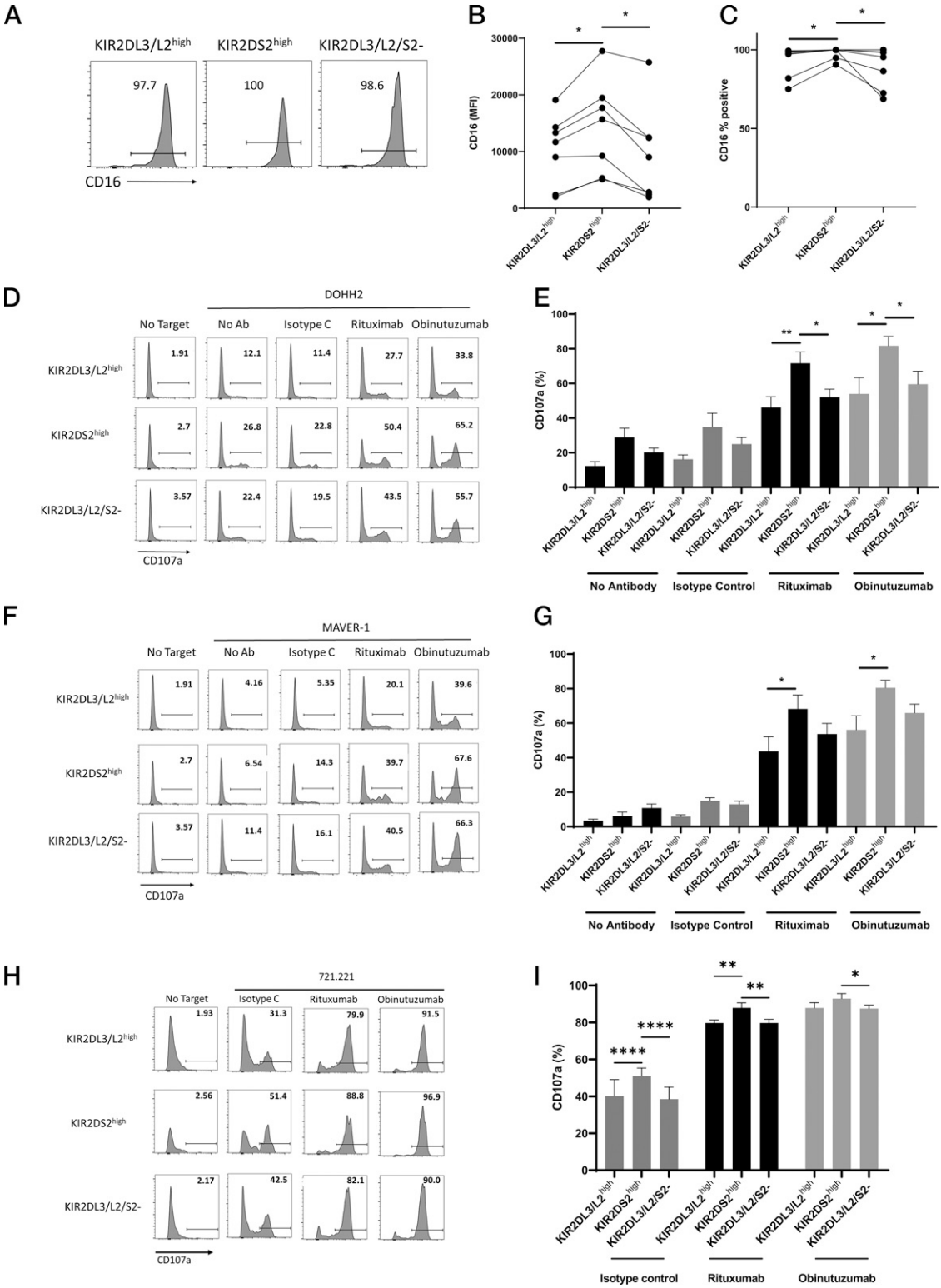

FIGURE 4. KIR2DS2^{high} NK cells have enhanced CD16 expression and response to anti-CD20 Abs. Expression of CD16 was assessed using flow cytometry on healthy human CD3^{-}CD56^{dim} NK cells. Representative plots are shown in (**A**), and summarized data from seven separate donors are shown in (**B**) as mean fluorescence intensity and in (**C**) as the percent positive. (**D–I**) Healthy human PBMCs were incubated with IL-15 (1 ng/ml) overnight and then cocultured with DOHH2 (D and E), MAVER-1 (F and G), or 721.221 (H and I) cells at a 10:1 E:T ratio or no target for 4 h in the presence of indicated Abs at 1 μg/ml concentration. CD107a expression was assessed on CD3^{-}CD56^{dim} NK cells separated into KIR2DS2^{high}, KIR2DL3/L2^{high}, or KIR2DL3/L2/S2^{-} populations. Representative plots are shown in (D), (F), and (H), and summarized are data shown in (E) ($n = 5$), (G) ($n = 5$), and (I) ($n = 7$). Data are presented as mean ± SEM. *$p < 0.05$, **$p < 0.01$, ****$p < 0.0001$.

compared with NK cells with low or absent expression of KIR2DS2. This was demonstrated by both enhanced natural cytotoxicity and ADCC against relevant target cells. Bulk RNA sequencing and a customized scRNAseq approach revealed that KIR2DS2^{+} NK cells are primed for activation, with a distinct transcriptional profile associated with NK cell–mediated cytotoxicity

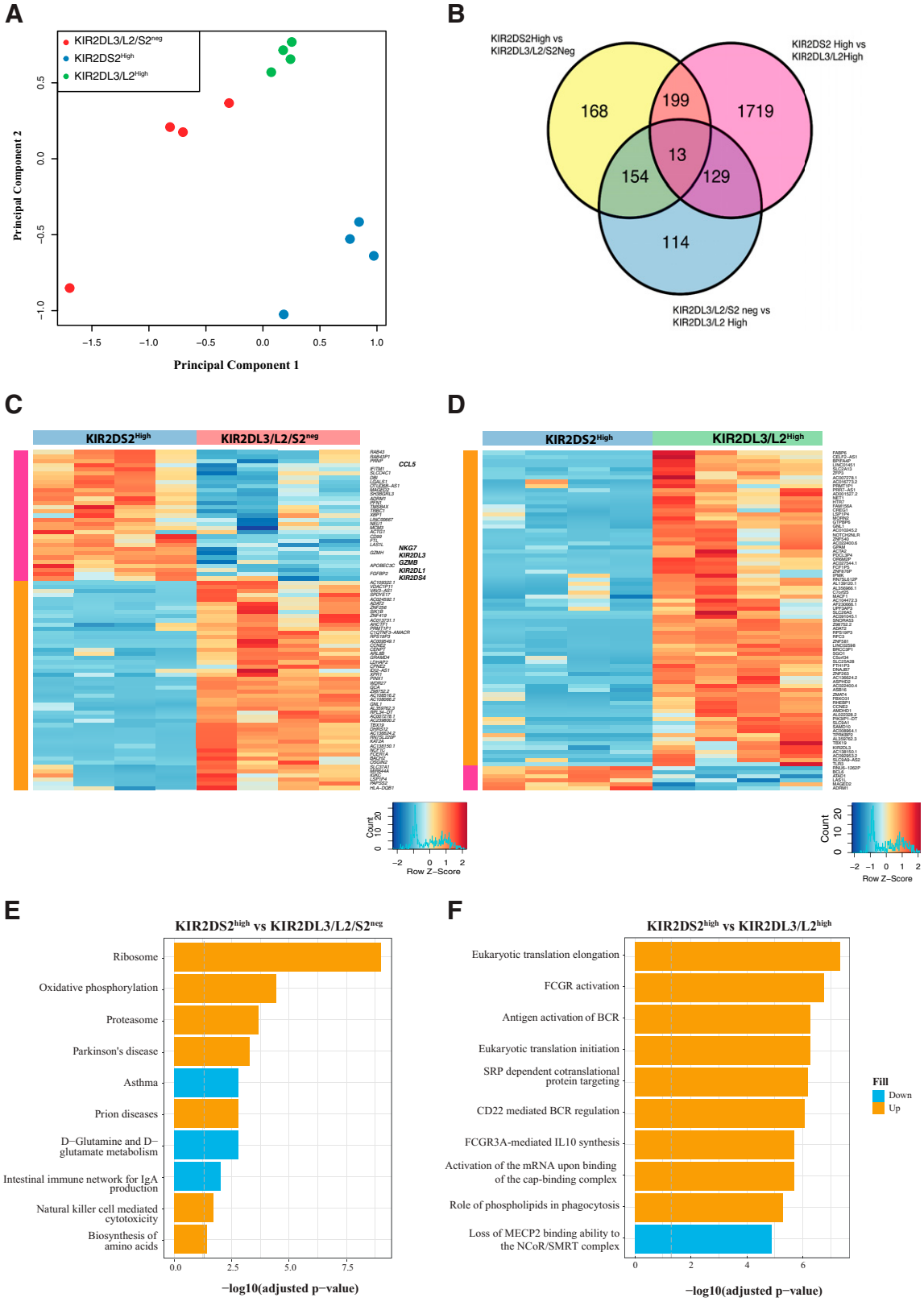

FIGURE 5. Bulk RNA sequencing identifies that KIR2DS2^{+} NK cells are primed for activation. Healthy human CD3^{-}CD56^{dim} NK cells were sorted using a BD FACSAria device into KIR2DS2^{high}, KIR2DL3/L2^{high}, or KIR2DL3/L2/S2^{-} populations and sequenced using an Illumina NovaSeq system. (**A**) Principal component analysis comparison of KIR2DS2^{high}, KIR2DL3/L2^{high}, and KIR2DL3/L2/S2^{-} NK cells. (**B**) Venn diagram comparing differential gene expression between KIR2DS2^{high}, KIR2DL3/L2^{high}, and KIR2DL3/L2/S2^{-} NK cells. False discovery rate <0.05 from the three contrasts analyzed. (**C** and **D**) Heatmaps showing differential gene expression compared between (C) KIR2DS2^{high} versus KIR2DL3/L2/S2^{-} and (D) KIR2DS2^{high} versus KIR2DL3/L2^{high}. The top 50 genes of each contrast are shown. Genes were clustered using Pearson correlation and ward.D2, and color intensity denotes the gene expression level. (**E** and **F**) Kyoto Encyclopedia of Genes and Genomes analysis showing significantly altered pathways between the different subsets of NK cells: (E) KIR2DS2^{high} versus KIR2DL3/L2/S2^{-} and (F) KIR2DS2^{high} versus KIR2DL3/L2^{high}. The top 10 enriched gene sets are plotted for each contrast. Blue bars show downregulated pathways, whereas orange bars represent upregulated pathways.

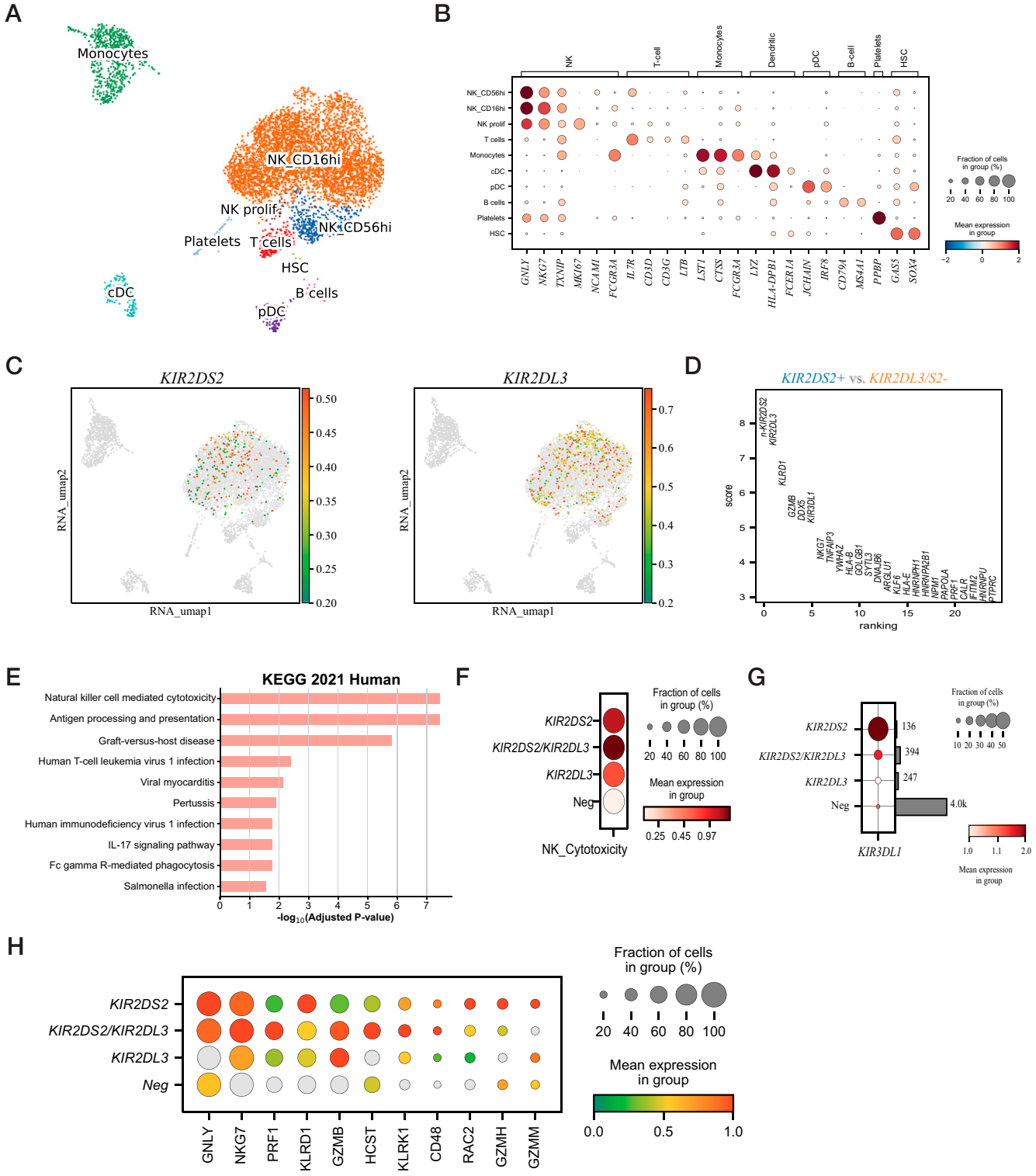

FIGURE 6. scRNAseq identifies that KIR2DS2 is significantly associated with NK cell–mediated cytotoxicity. NK cells from four donors were enriched using a negative selection kit. Single-cell transcriptome analysis was performed using the 3′ capture kit (version 3.1) from 10× Genomics. KIRs were pulled down from the full-length cDNA library using specific probes and subsequently sequenced using Nanopore. (**A**) Integrated Uniform Manifold Approximation and Projection (UMAP) plot from four donors (n = 6525 cells) showing the cluster annotation. (**B**) Rank gene analysis showing the marker genes used for cluster annotation. (**C**) Detection of KIR2DS2 and KIR2DL3 using long-read sequencing and mapping to the UMAP plot defined by short-read transcriptomics. (**D**) Differential gene expression comparing KIR2DS2^{+} versus KIR2DS2^{-} within the CD16^{hi} NK cell population. (**E**) Gene set enrichment analysis for the differentially expressed genes from the contrast KIR2DS2^{+} versus KIR2DS2^{-} within the CD16^{hi} NK cell population. Genes used for the analysis had false discovery rates <0.05. The Kyoto Encyclopedia of Genes and Genomes (KEGG) database (2021) was used for the enrichment analysis. The top 10 significant terms are shown. (**F**) Gene set enrichment analysis of the NK cytotoxicity gene set (KEGG) among the four NK subsets identified using long-read sequencing. Color scales represent mean Z-score. (**G**) KIR3DL1 gene expression among the four subsets identified using long-read sequencing. Color scales represent the mean of gene expression. Side bars show the number of cells in each category. (**H**) Individual gene expression of selected genes from the NK cytotoxicity gene set (KEGG) among four NK subsets identified using long-read sequencing.

and translational activity. Taken together, these results indicate that KIR2DS2$^+$ NK cells may potentially represent an attractive cellular entity for the development of future immunotherapeutic strategies.

KIR2DS2$^+$ donor cells are beneficial for the outcome of cord blood transplant for hematological malignancies, and KIR2DS2 is also associated with reduced incidence in the development of childhood ALL (19, 20). However, studies have not investigated this protection on a mechanistic level. One reason for this may have been the lack of reagents able to discriminate between KIR2DS2 and the closely related inhibitory KIRs KIR2DL3 and KIR2DL2. Previously, KIR2DS2$^+$ NK cells have been shown to possess enhanced cytotoxic and cytokine activity in response to the acute myeloid leukemia cell line K562 (20) and neuroblastoma cells in vitro and in vivo (21); however, these studies used Abs unable to differentiate between KIR2DS2 and the inhibitory KIRs KIR2DL2 and KIR2DL3. In this study, using a recently described flow cytometry assay implementing a novel Ab combination, we showed a marked difference in reactivity against cancer targets between KIR2DS2^{high} (KIR2DL3/L2^{low}) and KIR2DL3/L2^{high} NK cells, indicating that cells expressing these different combinations of receptors have discernible differences in function. Recent genetic analysis showed that the presence of KIR2DL2 and/or KIR2DS2 on donor NK cells and the absence of inhibitory KIR2DL1, KIR2DL3, and KIR3DL1 are associated with protection against relapse following stem cell transplant in patients with acute myeloid leukemia (46). However, KIR2DL2 and KIR2DS2 are in tight linkage disequilibrium, and therefore understanding this protection is not possible using an immunogenetic approach. The results from our study indicate that, at the functional level, KIR2DS2 and not KIR2DL2 is associated with enhanced reactivity against cancer cells and therefore is most likely to be the protective factor.

KIR2DS1 directly recognizes HLA-C2 on target leukemic cells (47); however, no cancer-associated ligands for KIR2DS2 have yet been identified. Using a reporter cell line, one study showed that KIR2DS2 can bind cancer cells in a β_2-microglobulin–independent manner; however, the ligand was not identified and also bound to KIR2DL3 (12). Thus, this mechanism is unlikely to be relevant to our observations. KIR2DS2 interacts with HLA-C (8, 10, 48) and with HLA-A*1101 (49); however, the data presented in this study indicate that KIR2DS2^{high} NK cells retain enhanced activation even in the absence of HLA-C on target cells, and thus this gene marks NK cells with general enhanced anticancer activity. This indicates that KIR2DS2 may be a promising target for intervention for tumors in which MHC class I downregulation contributes to therapy resistance (50). Blocking of HLA-C simultaneously releases inhibitory KIR-mediated inhibition and as such could not be used to probe the contribution of this interaction to NK cell activation. However, enhanced activation of KIR2DS2^{high} NK cells compared with KIR2DL3/L2^{high} cells was observed against targets in the absence of HLA-C, indicating that inhibition by KIR2DL3/L2 was not the driver of the difference between the subpopulations.

RNA sequencing revealed that KIR2DS2$^+$ NK cells have upregulation of pathways, including NK-mediated cytotoxicity and FCGR signaling, as well as pathways associated with translation and ribosome and oxidative phosphorylation. This supports the functional data and provides a mechanism whereby the enhanced effector functions of KIR2DS2^{high} NK cells are evoked. For example, oxidative phosphorylation is required for prolonged NK activation (51), and translational pathways are key for production of perforin and granzyme B during NK cytotoxic responses (52). Specific genes of interest upregulated included NKG7, which is critical for translocation of CD107a to the cell surface and delivery of cytotoxic molecules to target cells (53), in accordance with the functional data from this study showing enhanced degranulation in the KIR2DS2^{high} subset. In addition, the cell death–inducing enzyme, granzyme B, was upregulated in KIR2DS2$^+$ NK cells and is released by NK cells to eliminate target cells (54). Interestingly, CCL5 was upregulated in KIR2DS2$^+$ NK cells, and this chemokine recruits conventional type 1 dendritic cells into the tumor microenvironment (55, 56). The scRNA-seq data revealed that KIR2DS2$^+$ NK cells were more cytotoxic when KIR2DL3 was coexpressed. Although we could not assess coexpression of KIR2DL2 in this population because of high gene homology, the functional data indicate that KIR2DS2, but not KIR2DL3 or KIR2DL2, is associated with enhanced NK function. KIR2DL3 and potentially KIR2DL2 are required, at least at a low level, for the education and maximal cytotoxic potential of KIR2DS2$^+$ NK cells. Together, these data indicate that KIR2DS2 marks a population of NK cells that are primed at the transcriptional level for response against target cells. In addition, we provide proof of concept that RAGE-seq can be used to assess NK cells and KIRs. This technique could be developed in future work to assess the full repertoire of KIR expression by NK cells linked with the transcriptional profile of NK cells. This may prove useful to study KIR not only in cancer but also in infectious diseases and reproductive disorders for which KIRs are also strongly associated with outcome (6).

Ab-mediated targeting of tumor cells has revolutionized cancer therapy, with anti-CD20 Abs such as rituximab in particular defining a new paradigm for the treatment of B cell malignancies (27). The identification that KIR2DS2 marks a population of NK cells with increased CD16 expression and activation in response to anti-CD20 Abs may therefore allow new approaches to enhance responses. For example, donors with KIR2DS2 may be selected during adoptive NK cell transfer therapies in combination with anti-CD20 Abs. These data are in accordance with previous studies which identified that KIR2DS2 is associated with enhanced activation in response to tumor targeting Abs in neuroblastoma and glioblastoma patients (21, 29). Inhibitory KIR–HLA interactions have been shown to inhibit rituximab- but not obinutuzumab-induced ADCC (57), and the enhanced rituximab-induced ADCC in KIR2DS2^{high} compared with KIR2DL3/L2^{high} NK populations may therefore be due to reduced inhibitory KIR expression in the KIR2DS2^{high} population. In agreement with this, blocking inhibitory KIRs with anti-KIR Abs enhanced cytotoxicity against lymphoma cells in combination with anti-CD20 Abs (58). In contrast, obinutuzumab-induced ADCC is thought to be largely independent of inhibitory KIR–HLA interactions (57); however our findings indicate that obinutuzumab-induced activation of NK cells is enhanced in the presence of KIR2DS2. This may not have previously been recognized because of high homology between KIR2DS2 and KIR2DL3/L2 and the difficulties in detection of KIR2DS2 by flow cytometry or conventional RNA sequencing.

Therapeutic targeting of activating KIRs has been hampered by the lack of mAbs able to discriminate between activating and inhibitory KIRs. As such, therapeutic benefit of KIR2DS2$^+$ NK cells has to date been achieved through selection of KIR2DS2$^+$ donors during transplant. Alternatively, therapeutic targeting of KIR2DS2 may be achieved via viral peptide ligands for KIR2DS2 (59) or selection of KIR2DS2$^+$ donors in a chimeric Ag receptor–NK approach to harness native enhanced NK cell activity (60). In conclusion, our observations indicate that KIR2DS2$^+$ NK cells may be attractive cellular entities for therapeutic strategies against cancer, and further preclinical studies are now underway to assess this.

Acknowledgments

We thank Richard Jewel and Carolann McGuire for technical assistance with flow cytometry. We also thank all patients and volunteers who donated blood used in this study.

Disclosures

M.D.B., R.F., and S.I.K. have applied for a patent for peptide mediated NK cell activation. All other authors declare that they have no relevant conflicts of interest.

References

1. Chiossone, L., P. Y. Dumas, M. Vienne, and E. Vivier. 2018. Natural killer cells and other innate lymphoid cells in cancer. [Published erratum appears in 2018 Nat. Rev. Immunol. 18: 726.] *Nat. Rev. Immunol.* 18: 671–688.
2. Cerwenka, A., and L. L. Lanier. 2018. Natural killers join the fight against cancer. *Science* 359: 1460–1461.
3. Bald, T., M. F. Krummel, M. J. Smyth, and K. C. Barry. 2020. The NK cell-cancer cycle: advances and new challenges in NK cell-based immunotherapies. *Nat. Immunol.* 21: 835–847.
4. Sabry, M., and M. W. Lowdell. 2020. Killers at the crossroads: the use of innate immune cells in adoptive cellular therapy of cancer. *Stem Cells Transl. Med.* 9: 974–984.
5. Hilton, H. G., and P. Parham. 2017. Missing or altered self: human NK cell receptors that recognize HLA-C. *Immunogenetics* 69: 567–579.
6. Blunt, M. D., and S. I. Khakoo. 2020. Activating killer cell immunoglobulin-like receptors: detection, function and therapeutic use. *Int. J. Immunogenet.* 47: 1–12.
7. Pende, D., M. Falco, M. Vitale, C. Cantoni, C. Vitale, E. Munari, A. Bertaina, F. Moretta, G. Del Zotto, G. Pietra, et al. 2019. Killer Ig-like receptors (KIRs): their role in NK cell modulation and developments leading to their clinical exploitation. *Front. Immunol.* 10: 1179.
8. Stewart, C. A., F. Laugier-Anfossi, F. Vély, X. Saulquin, J. Riedmuller, A. Tisserant, L. Gauthier, F. Romagné, G. Ferracci, F. A. Arosa, et al. 2005. Recognition of peptide-MHC class I complexes by activating killer immunoglobulin-like receptors. *Proc. Natl. Acad. Sci. USA* 102: 13224–13229.
9. Yang, Y., H. Bai, Y. Wu, P. Chen, J. Zhou, J. Lei, X. Ye, A. J. Brown, X. Zhou, T. Shu, et al. 2022. Activating receptor KIR2DS2 bound to HLA-C1 reveals the novel recognition features of activating receptor. *Immunology* 165: 341–354.
10. Naiyer, M. M., S. A. Cassidy, A. Magri, V. Cowton, K. Chen, S. Mansour, H. Kranidioti, B. Mbiribindi, P. Rettman, S. Harris, et al. 2017. KIR2DS2 recognizes conserved peptides derived from viral helicases in the context of HLA-C. *Sci. Immunol.* 2: eaal5296.
11. Blunt, M. D., P. Rettman, L. Y. Bastidas-Legarda, R. Fulton, V. Capizzuto, M. M. Naiyer, J. A. Traherne, and S. I. Khakoo. 2019. A novel antibody combination to identify KIR2DS2^{high} natural killer cells in KIR2DL3/L2/S2 heterozygous donors. *HLA* 93: 32–35.
12. Thiruchelvam-Kyle, L., S. E. Hoelsbrekken, P. C. Saether, E. G. Bjørnsen, D. Pende, S. Fossum, M. R. Daws, and E. Dissen. 2017. The activating human NK cell receptor KIR2DS2 recognizes a β_2-microglobulin-independent ligand on cancer cells. *J. Immunol.* 198: 2556–2567.
13. Djaoud, Z., and P. Parham. 2020. HLAs, TCRs, and KIRs, a triumvirate of human cell-mediated immunity. *Annu. Rev. Biochem.* 89: 717–739.
14. Bachanova, V., D. J. Weisdorf, T. Wang, S. G. E. Marsh, E. Trachtenberg, M. D. Haagenson, S. R. Spellman, M. Ladner, L. A. Guethlein, P. Parham, et al. 2016. Donor KIR B genotype improves progression-free survival of non-Hodgkin lymphoma patients receiving unrelated donor transplantation. *Biol. Blood Marrow Transplant.* 22: 1602–1607.
15. Cooley, S., E. Trachtenberg, T. L. Bergemann, K. Saeteurn, J. Klein, C. T. Le, S. G. Marsh, L. A. Guethlein, P. Parham, J. S. Miller, and D. J. Weisdorf. 2009. Donors with group B KIR haplotypes improve relapse-free survival after unrelated hematopoietic cell transplantation for acute myelogenous leukemia. *Blood* 113: 726–732.
16. Cooley, S., D. J. Weisdorf, L. A. Guethlein, J. P. Klein, T. Wang, S. G. Marsh, S. Spellman, M. D. Haagenson, K. Saeturn, M. Ladner, et al. 2014. Donor killer cell Ig-like receptor B haplotypes, recipient HLA-C1, and HLA-C mismatch enhance the clinical benefit of unrelated transplantation for acute myelogenous leukemia. *J. Immunol.* 192: 4592–4600.
17. Weisdorf, D., S. Cooley, T. Wang, E. Trachtenberg, C. Vierra-Green, S. Spellman, J. A. Sees, A. Spahn, J. Vogel, T. A. Fehniger, et al. 2020. KIR B donors improve the outcome for AML patients given reduced intensity conditioning and unrelated donor transplantation. [Published erratum appears in 2022 *Blood Adv.* 6: 1536.] *Blood Adv.* 4: 740–754.
18. Hong, S., L. Rybicki, A. Zhang, D. Thomas, C. M. Kerr, J. Durrani, M. A. Rainey, A. Mian, T. R. Behera, H. E. Carraway, et al. 2021. Influence of killer immunoglobulin-like receptors and somatic mutations on transplant outcomes in acute myeloid leukemia. *Transplant. Cell. Ther.* 27: 917.e1–917.e9.
19. Almalte, Z., S. Samarani, A. Iannello, O. Debbeche, M. Duval, C. Infante-Rivard, D. K. Amre, D. Sinnett, and A. Ahmad. 2011. Novel associations between activating killer-cell immunoglobulin-like receptor genes and childhood leukemia. *Blood* 118: 1323–1328.
20. Sekine, T., D. Marin, K. Cao, L. Li, P. Mehta, H. Shaim, C. Sobieski, R. Jones, B. Oran, C. Hosing, et al. 2016. Specific combinations of donor and recipient KIR-HLA genotypes predict for large differences in outcome after cord blood transplantation. *Blood* 128: 297–312.
21. Gras Navarro, A., J. Kmiecik, L. Leiss, M. Zelkowski, A. Engelsen, Ø. Bruserud, J. Zimmer, P. O. Enger, and M. Chekenya. 2014. NK cells with KIR2DS2 immunogenotype have a functional activation advantage to efficiently kill glioblastoma and prolong animal survival. *J. Immunol.* 193: 6192–6206.
22. Cariani, E., M. Pilli, A. Zerbini, C. Rota, A. Olivani, P. Zanelli, A. Zanetti, T. Trenti, C. Ferrari, and G. Missale. 2013. HLA and killer immunoglobulin-like receptor genes as outcome predictors of hepatitis C virus-related hepatocellular carcinoma. *Clin. Cancer Res.* 19: 5465–5473.
23. Wiśniewski, A., R. Jankowska, E. Passowicz-Muszyńska, E. Wiśniewska, E. Majorczyk, I. Nowak, I. Frydecka, and P. Kuśnierczyk. 2012. KIR2DL2/S2 and HLA-C C1C1 genotype is associated with better response to treatment and prolonged survival of patients with non-small cell lung cancer in a Polish Caucasian population. *Hum. Immunol.* 73: 927–931.
24. Beksac, K., M. Beksac, K. Dalva, E. Karaagaoglu, and M. B. Tirnaksiz. 2015. Impact of "killer immunoglobulin-like receptor /ligand" genotypes on outcome following surgery among patients with colorectal cancer: activating KIRs are associated with long-term disease free survival. *PLoS One* 10: e0132526.
25. Alomar, S. Y., A. Alkhuriji, P. Trayhyrn, A. Alhetheel, A. Al-Jurayyan, and L. Mansour. 2017. Association of the genetic diversity of killer cell immunoglobulin-like receptor genes and HLA-C ligand in Saudi women with breast cancer. *Immunogenetics* 69: 69–76.
26. Seidel, U. J., P. Schlegel, and P. Lang. 2013. Natural killer cell mediated antibody-dependent cellular cytotoxicity in tumor immunotherapy with therapeutic antibodies. *Front. Immunol.* 4: 76.
27. Marshall, M. J. E., R. J. Stopforth, and M. S. Cragg. 2017. Therapeutic antibodies: what have we learnt from targeting CD20 and where are we going? *Front. Immunol.* 8: 1245.
28. Rudnicka, D., A. Oszmiana, D. K. Finch, I. Strickland, D. J. Schofield, D. C. Lowe, M. A. Sleeman, and D. M. Davis. 2013. Rituximab causes a polarization of B cells that augments its therapeutic function in NK-cell-mediated antibody-dependent cellular cytotoxicity. *Blood* 121: 4694–4702.
29. Siebert, N., C. Jensen, S. Troschke-Meurer, M. Zumpe, M. Jüttner, K. Ehlert, S. Kietz, I. Müller, and H. N. Lode. 2016. Neuroblastoma patients with high-affinity FCGR2A, -3A and stimulatory KIR 2DS2 treated by long-term infusion of anti-GD_2 antibody ch14.18/CHO show higher ADCC levels and improved event-free survival. *Oncoimmunology* 5: e1235108.
30. Bray, N. L., H. Pimentel, P. Melsted, and L. Pachter. 2016. Near-optimal probabilistic RNA-seq quantification. [Published erratum appears in 2016 *Nat Biotechnol*. 34: 888.] *Nat. Biotechnol.* 34: 525–527.
31. Pimentel, H., N. L. Bray, S. Puente, P. Melsted, and L. Pachter. 2017. Differential analysis of RNA-seq incorporating quantification uncertainty. *Nat. Methods* 14: 687–690.
32. Robinson, M. D., D. J. McCarthy, and G. K. Smyth. 2010. edgeR: a Bioconductor package for differential expression analysis of digital gene expression data. *Bioinformatics* 26: 139–140.
33. Ritchie, M. E., B. Phipson, D. Wu, Y. Hu, C. W. Law, W. Shi, and G. K. Smyth. 2015. limma powers differential expression analyses for RNA-sequencing and microarray studies. *Nucleic Acids Res.* 43: e47.
34. Alhamdoosh, M., M. Ng, N. J. Wilson, J. M. Sheridan, H. Huynh, M. J. Wilson, and M. E. Ritchie. 2017. Combining multiple tools outperforms individual methods in gene set enrichment analyses. *Bioinformatics* 33: 414–424.
35. Singh, M., G. Al-Eryani, S. Carswell, J. M. Ferguson, J. Blackburn, K. Barton, D. Roden, F. Luciani, T. Giang Phan, S. Junankar, et al. 2019. High-throughput targeted long-read single cell sequencing reveals the clonal and transcriptional landscape of lymphocytes. *Nat. Commun.* 10: 3120.
36. Lun, A. T. L., S. Riesenfeld, T. Andrews, T. P. Dao, T. Gomes, and J. C. Marioni; participants in the 1st Human Cell Atlas Jamboree. 2019. EmptyDrops: distinguishing cells from empty droplets in droplet-based single-cell RNA sequencing data. *Genome Biol.* 20: 63.
37. Wolf, F. A., P. Angerer, and F. J. Theis. 2018. SCANPY: large-scale single-cell gene expression data analysis. *Genome Biol.* 19: 15.
38. Macosko, E. Z., A. Basu, R. Satija, J. Nemesh, K. Shekhar, M. Goldman, I. Tirosh, A. R. Bialas, N. Kamitaki, E. M. Martersteck, et al. 2015. Highly parallel genome-wide expression profiling of individual cells using nanoliter droplets. *Cell* 161: 1202–1214.
39. Lebrigand, K., V. Magnone, P. Barbry, and R. Waldmann. 2020. High throughput error corrected Nanopore single cell transcriptome sequencing. *Nat. Commun.* 11: 4025.
40. Robinson, J., J. A. Halliwell, J. D. Hayhurst, P. Flicek, P. Parham, and S. G. Marsh. 2015. The IPD and IMGT/HLA database: allele variant databases. *Nucleic Acids Res.* 43: D423–D431.
41. Robinson, J., A. Malik, P. Parham, J. G. Bodmer, and S. G. Marsh. 2000. IMGT/HLA database – a sequence database for the human major histocompatibility complex. *Tissue Antigens* 55: 280–287.
42. a-slide/NanoCount 0.2.4.post1 Adrien Leger. Available at: https://zenodo.org/record/4486652#.Yo9K8u7TU2w. Accessed July 23, 2021.
43. Fisher, J. G., C. J. Walker, A. D. Doyle, P. W. Johnson, F. Forconi, M. S. Cragg, Y. Landesman, S. I. Khakoo, and M. D. Blunt. 2021. Selinexor enhances NK cell activation against malignant B cells *via* downregulation of HLA-E. *Front. Oncol.* 11: 785635.
44. Romee, R., M. Rosario, M. M. Berrien-Elliott, J. A. Wagner, B. A. Jewell, T. Schappe, J. W. Leong, S. Abdel-Latif, S. E. Schneider, S. Willey, et al. 2016. Cytokine-induced memory-like natural killer cells exhibit enhanced responses against myeloid leukemia. *Sci. Transl. Med.* 8: 357ra123.
45. Gang, M., N. D. Marin, P. Wong, C. C. Neal, L. Marsala, M. Foster, T. Schappe, W. Meng, J. Tran, M. Schaettler, et al. 2020. CAR-modified memory-like NK cells exhibit potent responses to NK-resistant lymphomas. *Blood* 136: 2308–2318.
46. Guethlein, L. A., N. Beyzaie, N. Nemat-Gorgani, T. Wang, V. Ramesh, W. M. Marin, J. A. Hollenbach, J. Schetelig, S. R. Spellman, S. G. E. Marsh, et al. 2021. Following transplantation for acute myelogenous leukemia, donor KIR Cen B02 better protects against relapse than KIR Cen B01. *J. Immunol.* 206: 3064–3072.
47. Pende, D., S. Marcenaro, M. Falco, S. Martini, M. E. Bernardo, D. Montagna, E. Romeo, C. Cognet, M. Martinetti, R. Maccario, et al. 2009. Anti-leukemia

activity of alloreactive NK cells in KIR ligand-mismatched haploidentical HSCT for pediatric patients: evaluation of the functional role of activating KIR and redefinition of inhibitory KIR specificity. *Blood* 113: 3119–3129.
48. David, G., Z. Djaoud, C. Willem, N. Legrand, P. Rettman, K. Gagne, A. Cesbron, and C. Retière. 2013. Large spectrum of HLA-C recognition by killer Ig-like receptor (KIR)2DL2 and KIR2DL3 and restricted C1 SPECIFICITY of KIR2DS2: dominant impact of KIR2DL2/KIR2DS2 on KIR2D NK cell repertoire formation. *J. Immunol.* 191: 4778–4788.
49. Liu, J., Z. Xiao, H. L. Ko, M. Shen, and E. C. Ren. 2014. Activating killer cell immunoglobulin-like receptor 2DS2 binds to HLA-A*11. *Proc. Natl. Acad. Sci. USA* 111: 2662–2667.
50. Garrido, F., N. Aptsiauri, E. M. Doorduijn, A. M. Garcia Lora, and T. van Hall. 2016. The urgent need to recover MHC class I in cancers for effective immunotherapy. *Curr. Opin. Immunol.* 39: 44–51.
51. O'Brien, K. L., and D. K. Finlay. 2019. Immunometabolism and natural killer cell responses. *Nat. Rev. Immunol.* 19: 282–290.
52. Fehniger, T. A., S. F. Cai, X. Cao, A. J. Bredemeyer, R. M. Presti, A. R. French, and T. J. Ley. 2007. Acquisition of murine NK cell cytotoxicity requires the translation of a pre-existing pool of granzyme B and perforin mRNAs. *Immunity* 26: 798–811.
53. Ng, S. S., F. De Labastida Rivera, J. Yan, D. Corvino, I. Das, P. Zhang, R. Kuns, S. B. Chauhan, J. Hou, X. Y. Li, et al. 2020. The NK cell granule protein NKG7 regulates cytotoxic granule exocytosis and inflammation. *Nat. Immunol.* 21: 1205–1218.
54. Chowdhury, D., and J. Lieberman. 2008. Death by a thousand cuts: granzyme pathways of programmed cell death. *Annu. Rev. Immunol.* 26: 389–420.
55. Böttcher, J. P., E. Bonavita, P. Chakravarty, H. Blees, M. Cabeza-Cabrerizo, S. Sammicheli, N. C. Rogers, E. Sahai, S. Zelenay, and C. Reis e Sousa. 2018. NK cells stimulate recruitment of cDC1 into the tumor microenvironment promoting cancer immune control. *Cell* 172: 1022–1037.e14.
56. Voshtani, R., M. Song, H. Wang, X. Li, W. Zhang, M. S. Tavallaie, W. Yan, J. Sun, F. Wei, and X. Ma. 2019. Progranulin promotes melanoma progression by inhibiting natural killer cell recruitment to the tumor microenvironment. *Cancer Lett.* 465: 24–35.
57. Terszowski, G., C. Klein, and M. Stern. 2014. KIR/HLA interactions negatively affect rituximab- but not GA101 (obinutuzumab)-induced antibody-dependent cellular cytotoxicity. *J. Immunol.* 192: 5618–5624.
58. Kohrt, H. E., A. Thielens, A. Marabelle, I. Sagiv-Barfi, C. Sola, F. Chanuc, N. Fuseri, C. Bonnafous, D. Czerwinski, A. Rajapaksa, et al. 2014. Anti-KIR antibody enhancement of anti-lymphoma activity of natural killer cells as monotherapy and in combination with anti-CD20 antibodies. *Blood* 123: 678–686.
59. Rettman, P., M. D. Blunt, R. J. Fulton, A. F. Vallejo, L. Y. Bastidas-Legarda, L. España-Serrano, M. E. Polak, A. Al-Shamkhani, C. Retiere, and S. I. Khakoo. 2021. Peptide: MHC-based DNA vaccination strategy to activate natural killer cells by targeting killer cell immunoglobulin-like receptors. *J. Immunother. Cancer* 9: e001912.
60. Mehta, R. S., and K. Rezvani. 2018. Chimeric antigen receptor expressing natural killer cells for the immunotherapy of cancer. *Front. Immunol.* 9: 283.